

STUDIES OF SPARK PLASMAS

Diploma Project

by

Lars Martinsson

Lund Reports on Atomic Physics, LRAP-66

Lund, 1986

Department of Physics
Lund Institute of Technology
P.O. Box 118, S-221 00 LUND
Sweden

<u>CONTENTS</u>	<u>PAGE</u>
INTRODUCTION	4
1. INTRODUCTION TO SPARKS AND PLASMAS	5
1.1 Qualitative description of a spark discharge	5
1.2 Detailed processes in the plasma	8
1.3 The radiative properties of a plasma	12
1.4 Equations governing the plasma state	18
2. THE INTERPRETATION OF INTERFEROGRAMS	21
2.1 The connection between fringe shifts and concentrations	22
2.2 Abel inversion	24
2.3 Refractivity of the plasma components	31
2.4 Evaluation of the two-wavelength interferograms	34

5.3	Criteria for the validity of complete L.T.E. in a homogeneous and time-independent plasma	99
5.4	Criteria for the validity of complete L.T.E. in a homogeneous and transient plasma	101
5.5	Criteria for the validity of complete L.T.E. in an inhomogeneous and time-independent plasma	103
5.6	Application of the criteria to the sparks in nitrogen	105
6.	ACKNOWLEDGEMENTS	110
7.	REFERENCES	111

1. INTRODUCTION TO SPARKS AND PLASMAS

This first chapter contains some introductory material which is necessary for the understanding of the subsequent chapters. In the first section the process of a spark discharge is described qualitatively. This is only a very rough outline intended to give a general feeling for which phase of the spark development the results presented in Chapter 4 belong. The essence of Sections 1.2 and 1.4 is that it is difficult to obtain a description of a plasma in general but it is very easy if the plasma is in thermodynamic equilibrium. It is also an introduction to the possible processes in a plasma, of which the radiative processes is described in Section 1.3. The considerations in these three sections are necessary as a background to the concept of local thermodynamic equilibrium which is introduced in Section 3.1.

1.1 Qualitative description of a spark discharge

A spark can be defined as a very short-lived electrical breakdown, in which a highly ionized plasma is produced from a weakly ionized gas. Its usefulness lies in the fact that it transforms electrical potential energy to highly concentrated thermal energy. Many different physical processes are involved in a spark breakdown depending on the temperature, pressure and the energy input, and they interact with each other in several complicated ways, but at least a quantitative description can be made without going into too much detail. To this

external circuitry limits the current or when the spark channel expansion limits the current density.

2. The hydrodynamic stage

A hot, luminous and highly ionized plasma channel has now been formed. The resistive heating also increases the pressure and, consequently, the channel expands radially outwards. The rate of this expansion is of the order of that of the thermal velocity of the atoms, and since the temperature in the spark channel is very high, the channel expansion is greater than the speed of sound and thus produces a shock wave. The temperature is higher between the channel and the shock front than in the surrounding gas, and very much higher in the channel. The gas density is low in the conducting channel and the bulk of the gas mass is pushed radially outwards. The energy of the channel is also dissipated by diffusion of the charged and excited particles, by thermal conduction and by radiation losses.

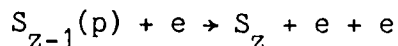
3. The cooling stage

When the energy supply is cut off the spark temperature falls, and the gas is deionized if the surrounding gas is inert. But if the surrounding gas consists of a combustible mixture a combustion wave can be on its way out from the spark. How combustion starts is still not quite clear.

This work is concerned with stage two above. Nothing will be said about the hydrodynamic properties of the plasma, only its atomic properties will be dealt with, although the interplay between these two domains is very important for an understanding of the behaviour of the spark. The atomic properties are amenable to experimental studies through the use of spectroscopic methods. Absorption and emission spectroscopy give quantitative knowledge of the species forming the plasma, their distribution over different quantum states and different ionization stages. Line shape measurements give knowledge of the electron density, gas temperature and of the ion temperature. It is important that the method of observation does not disturb the spark.

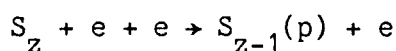
between an ion, S_Z , with charge Ze and an electron to form a new ion S_{Z-1} in a hydrogen plasma or in a hydrogenic plasma (reference [4]).

a) Collisional ionization



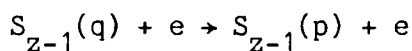
The ion S_{Z-1} is in quantum state p , and the rate coefficient for the reaction is $K(p, c^1)$, where c^1 is an energy level in the continuum of the free electrons, such that $n_e n_{Z-1} K(p, c^1)$ is the number of collisional ionization events that occurs in a unit volume element per second.

b) Three-body recombination

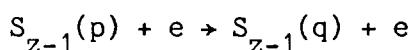


which is the inverse of (a) and it has the rate coefficient $K(c^1, p)$.

c) Collisional excitation, with the rate coefficient $K(q, p)$

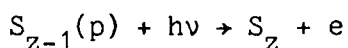


d) Collisional de-excitation



which is the inverse process to (c) and it has the rate coefficient $K(p, q)$

e) Photoionization



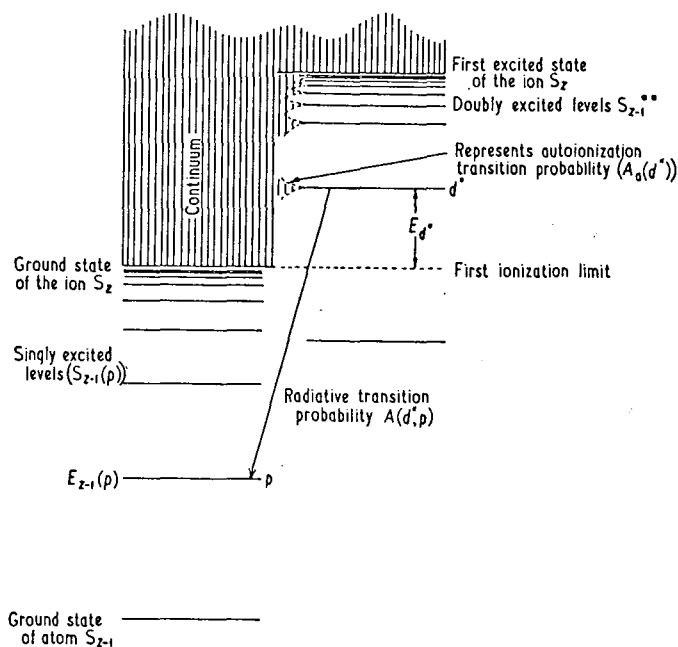
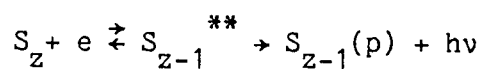


Figure 2.1. Schematic energy level diagram for a non-hydrogenic species of charge $z-1$ showing singly and doubly excited states, taken from reference [4].

The processes which are caused by atom-atom, atom-ion and ion-ion collisions are not included in the listing above, since their rates are much smaller than those for collisions with electrons in a plasma which is more than a few percent ionized.

The mechanisms above must be coupled to the radiation field in the plasma. The equations describing the field are quite complicated, but some solvable cases exist. In the next section introductory comments will be made about the radiation field.

There are three major types of radiation.

1. Bound-bound radiation

This type of radiation is emitted when an electron makes a transition between levels in an atom or an ion. The levels do not necessarily correspond exactly to those of an isolated atom, and the line profiles are also different. The emitted frequency ν is given by

$$h\nu = E(p) - E(q) \quad (3.1)$$

where $E(p)$ is the energy of quantum state p .

2. Free-bound (or recombination) radiation

This type of radiation is emitted when a free electron, i.e. an electron in the continuum, recombines with an ion. The electron may have any energy, and the radiation is therefore continuous; however, there is some structure due to the discrete nature of the bound states (absorption edges). If m_e is the electronic mass and v its velocity the frequency of the emitted radiation is given by

$$h\nu = E(\infty) + \frac{1}{2} m_e v^2 - E(p) \quad (3.2)$$

where $E(\infty)$ is the ionization energy.

3. Free-free radiation

Electronic transitions between two free energy levels can also occur in a plasma. Classically this is because a moving charge radiates when its velocity is changed. The two most common types of this radiation are bremsstrahlung, caused by the acceleration of charged particles in the electric field of other charged particles, and cyclotron spectra which arise from charged particles gyrating in a magnetic field. The major part of the bremsstrahlung comes from electron-ion collisions, and it has a continuous spectrum. The cyclotron spectrum, on the other hand, is discrete, for

The solution of equation (3.8) with the boundary condition that no radiation is incident at the boundary $x = D$, is

$$I(\nu, 0) = - \int_0^{\tau(\nu, D)} S(\nu, x) \exp\{-\tau'(\nu, x)\} d\tau'(\nu, x) \quad (3.9)$$

This is the radiation intensity that emerges at $x = 0$ from a plasma of depth D . This integration is quite complicated to perform. However, the result in some limiting cases may be stated explicitly. If the optical depth is small, that is

$$\tau(\nu, x) \ll 1 \quad (3.10)$$

then the intensity becomes

$$I(\nu, 0) = - \int_0^{\tau(\nu, D)} S d\tau = \int_0^D J(\nu, x) dx \quad (3.11)$$

This is known as the optical thin approximation, which is valid when the plasma is optically thin. On the other hand, if the optical depth is very large, an integration by parts of equation (3.9) gives

$$I(\nu, 0) = S(\tau=0) + \left. \frac{dS}{d\tau} \right|_{\tau=0} + \left. \frac{d^2S}{d\tau^2} \right|_{\tau=0} + \dots \quad (3.12)$$

and comparing with

$$S(\tau=1) = S_\nu(\tau=0) + \left. \frac{dS}{d\tau} \right|_{\tau=0} + \frac{1}{2} \left. \frac{d^2S}{d\tau^2} \right|_{\tau=0} + \dots \quad (3.13)$$

obtained from MacLaurin's theorem, it is seen that the intensity is roughly equal to the source function at an optical depth of $\tau=1$, if the higher order terms are small. In the last case the plasma is said to be optically thick.

emission and the probability per unit time that an atom emits a photon by this process is

$$B(p,q) I(\nu) \quad (3.14)$$

where $I(\nu)$ is the intensity of the radiation field

The total emission probability is then equal to

$$A(p,q) + B(p,q)I(\nu) \quad (3.15)$$

and the absorption probability per unit time is $B(q,p)I(\nu)$. If equilibrium conditions prevail, the principle of detailed balance may be invoked, and using the definitions above yields

$$n(q)B(q,p)I(\nu) = (A(p,q) + B(p,q)I(\nu)) n(p) \quad (3.16)$$

where $n(q)$ is the number density in state p .

But in thermodynamic equilibrium, the densities in different quantum states are governed by the Boltzmann distribution

$$\frac{n(p)}{n(q)} = \frac{g(p)}{g(q)} \exp \left\{ - \frac{h\nu_{pq}}{kT} \right\} \quad (3.17)$$

and the radiation intensity is given by Planck's radiation law

$$I(\nu) = \frac{2h\nu^3}{c^2} \left(\exp \left\{ \frac{h\nu}{kT} \right\} - 1 \right)^{-1} \quad (3.18)$$

Combining these relations leads immediately to

$$B(p,q) = \frac{g(q)}{g(p)} B(q,p) \quad (3.19)$$

and

absorption and emission coefficients will depend on the number densities in various quantum states and the atom or ion involved.

The situation is quite the opposite if the plasma happens to be in thermodynamic equilibrium. For a hot gas or a plasma to be in thermodynamic equilibrium it needs to be enclosed in a cavity with constant wall temperature. Then its physical state can be expressed by a finite number of thermodynamic variables, for instance the temperature, the pressure and the concentrations of its constituents. The temperature then gives the distribution of energy of any particular kind according to the Boltzmann distribution law

$$\frac{n_n}{n_m} = \frac{g_n}{g_m} \exp\left\{ -\frac{E_n - E_m}{kT} \right\} \quad (4.3)$$

where n_n is the number density in energy level n
 g_n is the statistical weight of level n
 E_n is the energy of level n
 k is Boltzmann's constant

In this case, for the number density in different energy states, the distribution over different ionization stages will be given by the Saha equation, the law of mass action for ionization (formula (3.3.20)). The velocity distribution for electrons, atoms and ions is then given by the Maxwell distribution

$$f_a(v)dv = \left(\frac{m_a}{2\pi kT}\right)^{3/2} v^2 \exp\left\{ -\frac{m_a v^2}{2kT} \right\} dv \quad (4.4)$$

where m_a is the mass of the particle.

The temperature of all the distributions is the same. The principle of detailed balance implies that in thermodynamic equilibrium the rates of the inverse processes in Section 1.2 are the same. Also, a radiative equilibrium must prevail, and then the intensity of the radiation is given by Planck's formula for radiation in a black-body cavity

2. THE INTERPRETATION OF INTERFEROGRAMS

One of the most useful experimental techniques to obtain information about the physical state of a spark is that of optical interferometry. To use electromagnetic radiation as a probe does not disturb the spark plasma, and the optical frequencies employed make it possible to observe the high electron concentrations that exist in the spark. The different diagnostic methods used in plasma physics are described in reference [7], and in particular the use of interferometry is described in references [19] and [20]. When two-wavelength interferometry is employed, the different frequency dependence of the refractivity of the plasma components permits a simultaneous determination of the concentrations of "particles" (molecules, atoms and ions) and that of electrons. Many such experiments have been performed on sparks (e.g. references [21] and [22]). In particular, the results from the experiment carried out by Aldén et al. (reference [1]), in which ultra-short, high-current sparks were produced in a nitrogen atmosphere, will be used in the numerical calculations in this report. The question of how to interpret the interferometric images recorded in this experiment, and how to calculate the electron and particle concentrations from them will be treated in this chapter.

The outline of the chapter is as follows. Section 2.1 deals with the relation between the fringe shifts and the number densities of electrons and particles, and Section 2.2 describes how this integral equation is numerically inverted for a cylindrically symmetric spark. To use this expression the refractivities of the plasma components must be known, and this will be the topic of Section 2.3. Finally, in

$$\mu-1 = \sum_i K_i n_i \quad (1.3)$$

where K_i is the specific refractivity of component i and n_i is the number density of component i .

In the case of the atmosphere consisting of a single species diatomic gas, this can be written as

$$\mu-1 = K_e n_e + K_m n_m + K_a n_0 + K_1 n_1 + K_2 n_2 + \dots \quad (1.4)$$

where the subscript

e	denotes electrons
m	" molecules
a,0	" atoms
1	" ions of charge -1
2	" ions of charge -2

If the interferometric measurement of the refractive index is made with the gas at room temperature and atmospheric pressure as a reference there will be negligible molecular dissociation and ionization. The expression for the reference refractive index will then be

$$\mu_0-1 = K_m n_u \quad (1.5)$$

where the undisturbed molecular number density, n_u , is calculated from the ideal gas law to be

$$n_u = 9.657 \times 10^{18} \frac{p[\text{torr}]}{T [\text{K}]} \quad [\text{cm}^{-3}] \quad (1.6)$$

where p and T are the pressure and temperature, respectively, in the undisturbed atmosphere.

Combining formulae (1.4) and (1.5) gives the expression for the difference in refractive index as

$$dx = \frac{r}{(r^2 - y^2)^{1/2}} dr \quad (2.2)$$

and

$$x = (R^2 - y^2)^{1/2} \quad (2.3)$$

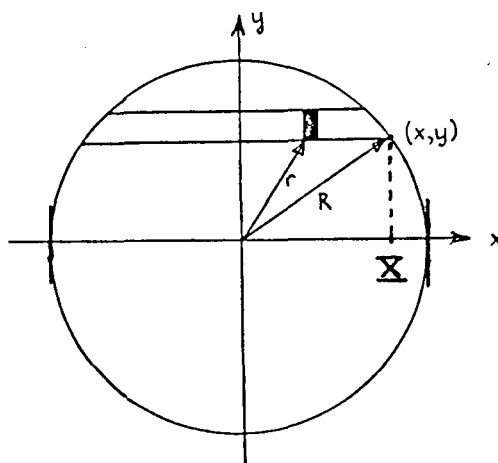


Figure 2.1. Geometrical relationships between the variables in the text.

Inserting these into equation (2.1) and using the symmetry about the y-axis yields

$$\Delta F(y) = \frac{2}{\lambda} \int_0^R \frac{\Delta \mu(r) r}{y (r^2 - y^2)^{1/2}} dr \quad (2.4)$$

Equation (2.4) is one of the forms of an Abel integral equation.

If $\mu(r)$ is assumed to be equal to zero for $r > R$, then it is possible to invert equation (2.4) analytically to give

described.

Equation (2.6) can be divided into two parts

$$F(r) = 2 \int_r^R \frac{\Delta F(y) y}{(y^2 - r^2)^{1/2}} dy \quad (2.7)$$

and

$$\Delta\mu(r) = - \frac{\lambda}{2\pi r} \frac{dF(r)}{dr} \quad (2.8)$$

The method requires that the relative fringe shift values should be measured at equidistant intervals, i.e. at the points

$$y_n = n\Delta \quad (2.9)$$

where the different n are integers in the range

$$0 \leq n \leq N \quad (2.10)$$

and the upper bound given by

$$N = \frac{R}{\Delta} \quad (2.11)$$

Consequently, the Abel-inverted fringe shift values will then be calculated at the points

$$r_n = n\Delta \quad (2.12)$$

From the measured relative fringe shift values, ΔF_n , a fringe shift function, $\Delta F(y)$, is now constructed by assuming that this function can be approximated by second-order polynomials between the measured points

$$\Delta F(y) = a_n + b_n y^2 \quad \text{when} \quad y_n \leq y \leq y_{n+1} \quad (2.13)$$

Equation (2.17) is now substituted into equation (2.8) and the result is

$$\begin{aligned}\Delta\mu(r_k) &= -\frac{\lambda}{2\pi\Delta^2 k} \frac{dF(k)}{dk} = \\ &= -\frac{\lambda}{\pi\Delta} (B_k + 2C_k k^2)\end{aligned}\quad (2.18)$$

The combination of the two coefficients, B_k and C_k is of the form

$$B_k + 2C_k k^2 = \begin{cases} -\sum_{n=k-2}^N \beta_{kn} \Delta F_n & \text{when } k \geq 2 \\ -\sum_{n=0}^N \beta_{kn} \Delta F_n & \text{when } k < 2 \end{cases} \quad (2.19)$$

where the β_{kn} coefficients are calculated numerically and depends on k and n through the α_{kn} coefficients, and they are independent of the value of N .

Combining equations (2.18) and (2.19) gives the final formula, the Abel inversion formula

$$\Delta\mu_k = \Delta\mu(r_k) = \begin{cases} \frac{\lambda}{\pi\Delta} \sum_{n=k-2}^N \beta_{kn} \Delta F_n & \text{when } k \geq 2 \\ \frac{\lambda}{\pi\Delta} \sum_{n=0}^N \beta_{kn} \Delta F_n & \text{when } k < 2 \end{cases} \quad (2.20)$$

In the coefficients β_{kn} lies the entire process of integration, least-squares fitting and the final differentiation. The values of the β_{kn} coefficients are presented in Table 2.1.

The four-figure accuracy of the coefficients is sufficient because, as well as the result of the inversion being insensitive to small random errors in the ΔF_n values, the result is also insensitive to small rounding-off errors in the β_{kn} values.

Barr recommends that this method be used when the uncertainty in the input data is of the order of one percent.

Finally it should be mentioned that because the β_{kn} coefficients are obtained by fitting the $F(k)$ polynomial (equation (2.17)) to a gaussian curve, the final values of the inversion for small k are smaller than the real values and in the wing (high k) the resulting values are slightly higher than the real values.

2.3 Refractivity of the plasma components

In the preceding section the procedure for calculating the variation of the refractive index as a function of the radial coordinate from the measured fringe shift values was outlined. Using equation (1.3) it is then possible to calculate the number densities of some of the plasma components, if the refractivities are known and additional assumptions are made about the state of the plasma. The expressions for the required refractivities of nitrogen and free electrons will be presented in this section. The material is collected from references [19], [20], [26] and [27].

Both classical and quantum physics agree on the expression for the refractive index

$$\mu - 1 = \frac{e^2}{3\epsilon_0 m_e} \sum_l n(l) \sum_k \frac{f_{lk}}{\omega_{lk}^2 - \omega^2} \quad \text{if } \omega \neq \omega_{lk} \quad (3.1)$$

where $n(l)$ is number density of atoms in quantum state l

m_e the electronic mass

f_{lk} the oscillator strength for transitions between quantum states l and k

ω_{lk} the angular frequency of the line corresponding to the transition from l to k

The refractivity for nitrogen atoms and ions can be expressed in the same way, with other values of the constants A_i and B_i , but since they are not needed in the subsequent treatment, their values will not be given here. It is sufficient to know that the ratio of the atomic refractivity to the molecular refractivity is

$$R = \frac{K_a}{K_m} \approx 0.63 \quad (3.4)$$

for nitrogen. R is assumed to be independent of the wavelength.

The dominating contribution to the plasma refractivity comes from the free electrons. If the angular frequency of the impinging radiation is much greater than the electron plasma frequency

$$\omega_p = \left(\frac{n_e e^2}{\epsilon_0 m_e} \right)^{1/2} = 5.64 \times 10^4 (n_e [\text{cm}^{-3}])^{1/2} \quad (3.5)$$

then the refractive index of the free electrons is

$$\begin{aligned} \mu_e - 1 &= K_e n_e = - \frac{e^2}{2\epsilon_0 m_e} \frac{1}{\omega^2} n_e \\ &= c_e n_e \lambda^2 \\ &= - 4.48 \times 10^{-14} n_e [\text{cm}^{-3}] (\lambda [\text{cm}])^2 \end{aligned} \quad (3.6)$$

This has the opposite sign to the atomic and molecular refractivities and a much stronger wavelength dependence than they have. The refractivities for nitrogen molecules, atoms and free electrons are shown in Figure 3.1

$$(\Delta F_k)_1 \equiv \mu_{k,1}$$

and $k = 0, 1, 2, \dots, 20$

$$(\Delta F_k)_2 \equiv \mu_{k,2}$$

where the numerical subscripts denote the wavelength. These can now be used to express the particle number densities according to equation (1.7), as

$$\Delta\mu_{k,1} = K_{e,1} n_{e,k} + K_{m,1} (n_{m,k} - n_u) + K_{a,1} n_{0,k} + K_{1,1} n_{1,k} + \dots \quad (4.1a)$$

$$\Delta\mu_{k,2} = K_{e,2} n_{e,k} + K_{m,2} (n_{m,k} - n_u) + K_{a,2} n_{0,k} + K_{1,2} n_{1,k} + \dots \quad (4.1b)$$

Dividing these equations by $K_{m,i}$ ($i=1$ and 2 , respectively), using relation (3.4) and assuming that the refractivities for atoms and ions are approximately the same, i.e.

$$K_a \approx K_1 \approx K_2 \approx \dots \quad (4.2)$$

give the equations

$$\frac{\Delta\mu_{k,1}}{K_{m,1}} = \frac{K_{e,1} n_{e,k}}{K_{m,1}} + n_{m,k} - n_u + R(n_{0,k} + n_{1,k} + \dots) \quad (4.3a)$$

$$\frac{\Delta\mu_{k,2}}{K_{m,2}} = \frac{K_{e,2} n_{e,k}}{K_{m,2}} + n_{m,k} - n_u + R(n_{0,k} + n_{1,k} + \dots) \quad (4.3b)$$

Dropping the second subscript on the molecular refractivity, since its wavelength dependence is very weak, and using the notation

$$\Delta N_k = n_{m,k} - n_u + R(n_{0,k} + n_{1,k} + \dots) \quad (4.4)$$

and solving for $n_{e,k}$ and ΔN_k yields the expression for the electron number density as

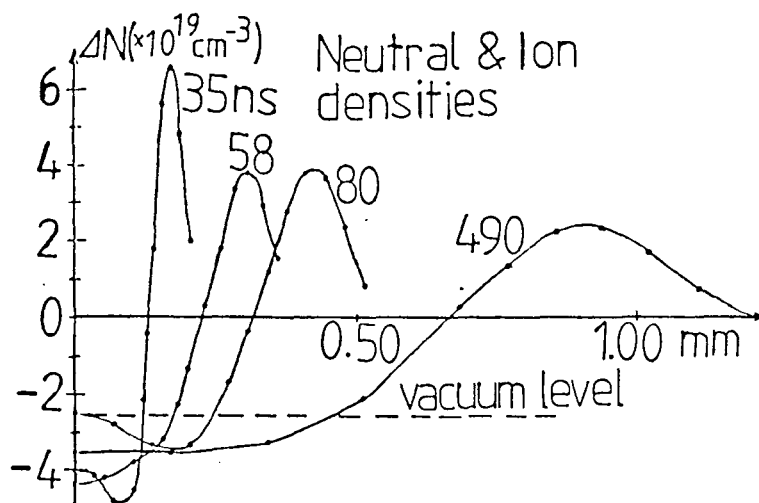


Figure 4.2. The particle number density versus radial distance for different times in sparks in nitrogen, taken from reference [1].

In Figure 4.2 the vacuum value is indicated. The distressing fact that the values of ΔN are below this level is explained by the fact that the expressions for the refractivities are not correct for the temperatures of the innermost regions of these sparks.

Alternatively, the order of Abel inversion and the algebraic manipulation could be reversed. In equations (4.5) and (4.6) the difference in refractive index, $\Delta\mu$, should then be replaced by the relative fringe shift, ΔF , and the expressions on the right-hand side should then be Abel-inverted. This might lead to different values of the concentrations due to numerical effects in the computations.

3.1 The concept of Local Thermodynamic Equilibrium

The most general way to obtain a description of the state of the spark plasma would be to set up the appropriate rate equations, exemplified in Section 1.4, and then to solve this system of equations. The solution could then be correlated with the experimental results to give the values of important physical parameters, such as the temperature or the number densities in different ionization stages. However, since most of the rate coefficients are not sufficiently well determined and the computational difficulties forbidding, especially the treatment of the radiative transfer, this approach would not yield any useful results for a nitrogen plasma.

If the spark could be considered to be in thermodynamic equilibrium at each instant it would be possible to obtain expressions describing the state of the plasma. But all laboratory plasmas lose energy through radiation and heat conduction to their surroundings and, consequently, cannot be in complete thermodynamic equilibrium. However, if some conditions are fulfilled, which will be stated explicitly in Chapter 5, the state of the spark can be very near that of complete equilibrium. This state is called Local Thermodynamic Equilibrium, in the following abbreviated to L.T.E. This concept of L.T.E. comes from plasma spectroscopy which deals with the radiation that is emitted from plasmas. In the book by Griem (reference [4]) L.T.E. is described thus. "Whenever L.T.E prevails, the densities in specific quantum states are those pertaining to a system in complete thermodynamic equilibrium, which has the same total (mass) density, temperature, and chemical composition as the actual system." (p. 130). With this very useful concept it is possible to obtain information about the state of the plasma without having to resort to complicated computations, and if the conditions for L.T.E are found not to hold, the results could serve as a first approximation to the non-equilibrium state that then exists.

of free electrons should be so high that collisions involving electrons will dominate over the radiative processes. The fulfilment of this condition is equivalent to the electrons having a maxwellian velocity distribution, equation (1.4.4) with the temperature, T , replaced by the the kinetic temperature of the electrons, T_e . This new temperature is essentially a parameter in the velocity distribution of the electrons, and only has a formal connection with the meaning of temperature in real life. The requirement that the electrons should be in thermal equilibrium with each other imposes new conditions on the spark; conditions that are not only local. They are that the mean free paths for electronic collisions should be much smaller than the geometrical dimensions of the plasma, and that the time between collisions must be short compared with other characteristic times, e.g. the time for particle heating and containment. Usually, the electron-electron mean free path and collisional relaxation times follow these prescriptions.

The atoms and ions may also have a maxwellian velocity distribution, but their kinetic temperatures need not be the same as the electronic kinetic temperature. For L.T.E. to hold, the kinetic temperatures should not be too different, say within 5% of each other. For plasmas which are not in L.T.E. especially the ions can have velocity distributions which are not thermal. Instead, the average kinetic energy W_i of any particular ion i is then a function of its charge Z and mass M , i.e.

$$W_i = f(Z, M) \neq kT_e \quad (1.1)$$

The function f can be determined experimentally from the Doppler widths of the spectral lines. The function reveals something about the power spectrum of the electric fields accelerating the ions, and this depends on the general dynamical behaviour and the relaxation processes in the plasma (reference [29]).

The radiative effects are assumed to be negligible when the plasma is in a state of L.T.E. The populations of quantum states are completely determined by collisional effects alone and, in rate equation language, the equations of radiative transfer are uncoupled

For a low density, optically thin plasma the photoexcitation processes are not important, and the radiative decay rates dominate over collisional decay rates. The electron densities are too low for L.T.E. or partial L.T.E. to exist, but another kind of equilibrium or quasi-steady state may be set up. The population of the excited levels will now be governed by an approximate equilibrium between the collisional excitation and the spontaneous emission processes. These are the conditions which exist in the solar corona, hence the name for this state is coronal equilibrium. For this state the thermodynamic equilibrium relations are inapplicable. According to Wilson [29] the populations of the levels below the level p (the thermal limit) in the partial L.T.E. situation can be calculated using this approximation.

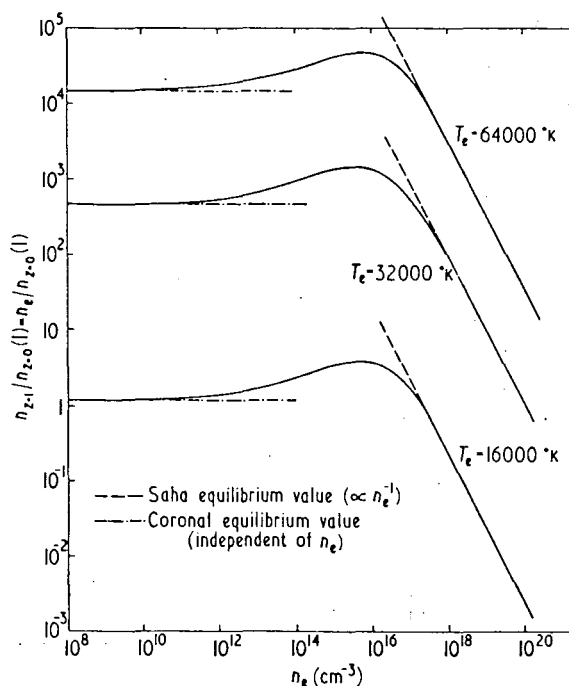


Figure 1.1. Illustration of the relation between the L.T.E. domain and the coronal domain for an optically thin hydrogen plasma, from reference [30].

For non-thermal plasmas the concept of temperature becomes questionable, or even meaningless, since the energy is not distributed over the different excited states according to the Boltzmann distribution. Neither are the velocity distributions maxwellian, nor is each collision process any longer balanced by its inverse process.

physics see references [31] and [32].) The quantities which can be considered as known from the beginning are the total number densities of the various elements, N_i , and the electron temperature, T_e . The thermodynamic potential which has an extremum for an equilibrium system with fixed volume and mass, i.e. fixed density, is the free energy, F . The connection between the free energy and the atomic properties, which will be the starting relation for the derivation of Saha's equation, is

$$F = - kT_e \ln Q \quad (2.1)$$

where k is Boltzmann's constant

Q is the total partition function for the system

T_e is the electron temperature

The electron temperature should be used here because the equilibrium is maintained by collisions with electrons

In the limit of no interaction between the plasma particles, except the necessary electron-ion collisions, equation (2.1) can be written

$$F_0 = - kT_e \ln Q_{fr} \quad (2.2)$$

where the subscript "fr" and denotes no interactions. The total partition function Q_{fr} is the product of the partition functions of the individual particles in the system, in this case an atom and the ions formed from the atom and the free electrons

$$Q_{fr} = Q_e \prod_{i=0}^z Q_i \quad (2.3)$$

where Q_e is the partition function for free electrons

Q_i is the partition function for ions in ionization stage i

z is the maximum ionization of the atom

The atomic and ionic partition function is

$$Q_i = \frac{(U_i)^{N_i}}{N_i!} \quad (2.7)$$

where U_i is the partition function of one single atom
(or ion) with charge i

N_i is the total number of such atoms (or ions)

The U_i 's are divided into a translational part, T_i , and an internal part B_i ;

$$U_i = T_i B_i \quad (2.8)$$

where the internal part is given as

$$B_i = \sum_l g_i(l) \exp \left\{ - \frac{E_i(l)}{kT_e} \right\} \quad (2.9)$$

a sum over all possible quantum levels l , with energy $E(l)$ and the statistical weight

$$g_i(l) = 2J_l + 1 \quad (2.10)$$

where J_l is the total angular momentum
of the atom in quantum state l

Collecting the expressions above into equation (2.2) yields a relation between the free energy of the plasma and the total number of electrons and the total number of atoms and ions. In order to be able to obtain a relation between the number densities in two successive ionization stages, consider now the ionization equilibrium



where the different single partition functions are related to the same ground level for the energy.

Substitution of the expressions (2.4) and (2.8) for the different U_i s into (2.16), and if the energy levels are referred to their respective ground states of the individual species, and also setting the translational part of the partition functions for S_i and S_{i-1} equal to each other, gives

$$\frac{n_i n_e}{n_{i-1}} = 2 \left(\frac{2\pi m_e kT_e}{h^2} \right)^{3/2} \frac{B_i(T_e)}{B_{i-1}(T_e)} \exp \left\{ - \frac{E_{i-1}(\infty)}{kT_e} \right\} \quad (2.17)$$

where $E_{i-1}(\infty)$ is the ionization energy of the species S_{i-1}

This equation is known as Saha's equation for a multicomponent system in thermodynamic equilibrium.

It is also possible to replace the total number density of an ionization level with the number density in an excited state of a specific ionization level by using the Boltzmann distribution formulae

$$\frac{n_i(a)}{n_i(b)} = \frac{g_i(a)}{g_i(b)} \exp \left\{ - \frac{E_i(a) - E_i(b)}{kT_e} \right\} \quad (2.18)$$

and

$$\frac{n_i(a)}{n_i} = \frac{g_i(a)}{B_i(T_e)} \exp \left\{ - \frac{E_i(a)}{kT_e} \right\} \quad (2.19)$$

where $n_i(a)$ is the number density of atoms (ions) i times ionized in quantum level a

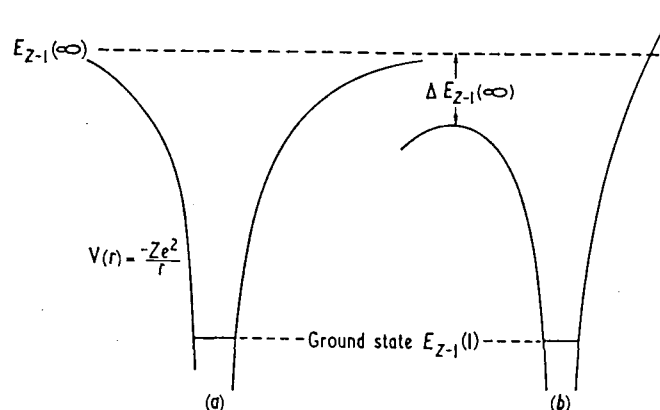


Figure 2.1. Representation of the potential around an atomic nucleus, (a) without and (b) with a constant external electric field, from reference [6].

The additional complication, the introduction of this effect into the Saha equation, is alleviated by the fact that it is a remedy against the formally infinite value of the internal partition function. For a free atom or ion the internal part of the partition function is a divergent sum over an infinite number of quantum levels. This divergence is prevented as there will now be a finite highest quantum number before the atom is ionized. This is true if the energy levels of the atom are considered to be unperturbed by this plasma interaction. The calculation of this lowering of the ionization energy of the ions in a plasma is treated in the next section.

3.3 The Saha equation II : Coulomb interactions and Debye theory

Since a particle in a plasma is surrounded by charged neighbours the electrical correlations between the particles have to be included in the expression for the free energy to give a better description of the plasma. This is accomplished by introducing an additional factor into the expression for the partition function for the whole system.

$$\Delta E_{i-1}(\infty) = -\left(\frac{\partial F_{\text{coul}}}{\partial N_e} - \frac{\partial F_{\text{coul}}}{\partial N_{i-1}} + \frac{\partial F_{\text{coul}}}{\partial N_i} \right) \quad (3.6)$$

Instead of using the expression (3.1) directly to calculate the Coulomb free energy with equation (3.3) another route will be followed. With the aid of the Debye approximation the average Coulomb interaction energy in the plasma can be calculated. From this it is possible to obtain the Coulomb free energy through the thermodynamic relation

$$F_{\text{coul}} = U_{\text{coul}} + \frac{\partial F_{\text{coul}}}{\partial T} T \quad (\text{if } dV=0) \quad (3.7)$$

where U_{coul} is the inner energy of the Coulomb interaction.

The Debye theory describes the screening effects in a plasma caused by the mobility of the charged particles. Inside the plasma the average charge density should be, on a macroscopic scale, equal to zero, if macroscopic charge neutrality is assumed. However, there will always be fluctuations around this average value in a small volume around a given charge. In order to calculate the radius of the sphere in which the charge density is appreciably different from zero, we put a point charge q at the origin and calculate the time-averaged and smoothed electrical potential outside the charge that is caused by the charge itself and the adjacent particles in the plasma. Since the plasma is assumed to be in equilibrium, the radial number density distribution function for the charged particles should be a canonical distribution (reference [3] or [36]). If the Coulomb interaction energy is small compared with the thermal energy this will give

$$n_i(r) = n_i \exp \left\{ - \frac{i e V_q(r)}{kT_e} \right\} \approx n_i \left(1 - \frac{i e V_q(r)}{kT_e} \right) \quad (3.8)$$

where $i = -1, 0, 1, 2, \dots$ (-1 is for electrons)

e is the elementary charge

$V_q(r)$ is the electrical potential

From equation (3.12) it can be seen that the electric field is split into two parts; for $r < r_D$ it is a Coulomb field and for $r > 2r_D$ the electric field is essentially zero, i.e. two charges which are further away than this have a negligible effect on each other.

The electrical interaction energy for the charge q then becomes

$$\begin{aligned}
 E_{el,q} &= 4\pi \int V_q(r) \rho_q(r) r^2 dr = \\
 &= - \frac{q^2 e^4}{4\pi \epsilon_0^2 kT_e} (n_e + \sum_i i^2 n_i) \int \exp\{-\frac{2r}{r_D}\} dr \quad (3.14) \\
 &= - \frac{q^2 e^2}{8\pi \epsilon_0 r_D}
 \end{aligned}$$

and, consequently the total internal energy contribution from the Coulomb interaction is

$$\begin{aligned}
 U_{coul} &= \sum_q N_q E_{el,q} = - \frac{e^2 V}{8\pi \epsilon_0 r_D} (n_e + \sum_i i^2 n_i) \\
 &= - \frac{e^3 V}{8\pi \epsilon_0^{3/2} (kT)^{1/2}} (n_e + \sum_i i^2 n_i)^{3/2} \quad (3.15)
 \end{aligned}$$

Substitution of this expression into (3.7) gives the Coulombic free energy as

$$F_{coul} = - \frac{2}{3} \frac{e^3 V}{8\pi \epsilon_0^{3/2} (kT)^{1/2}} (n_e + \sum_i i^2 n_i)^{3/2} \quad (3.16)$$

and, finally, substitution into (3.6) gives the lowering of the ionization energy as

The uncertainty in the exponential term in the Saha equation can be estimated by considering the Debye theory as a power series expansion of the ionization energy in terms of the ratio of the reduction of the ionization energy to the thermal energy. This implies that an error of the magnitude

$$\left(\frac{\Delta E(\infty)}{kT_e} \right)^2$$

should be expected even if the condition expressed by equation (3.18) is fulfilled.

3.4 The Saha equation III : calculation of the internal partition functions

In the final expression for the Saha equation above, formula (3.20), one thing still remains to be accounted for, and that is how to calculate the internal partition functions. This will be treated in this section.

The expression for the internal partition function was given earlier as (equation (2.9))

$$B_{i-1}(T_e) = \sum_l g_{i-1}(l) \exp\left\{ -\frac{E_{i-1}(l)}{kT_e} \right\} \quad (4.1)$$

where $g_{i-1}(l)$ is the statistical weight of the level represented by the set of quantum numbers l , usually (equation (2.10))

$$g_{i-1}(l) = 2J_l + 1 \quad (4.2)$$

and $E_{i-1}(l)$ is the energy of the level.

where E_H is the ionization energy of a free hydrogen atom

In principle, a direct summation up to the reduced ionization limit could now be performed with the aid of a table over atomic energy levels, for instance Moore (reference [39]). But the list of energy levels almost always becomes incomplete before the maximum orbital quantum number is reached. Also, for most higher levels the data for high angular momentum quantum numbers are not included in the tables. Since these levels have high statistical weights, their omission leads to a serious error in the excited-state contribution to the partition function. To overcome this difficulty, the summation is performed over the tabulated configurations for which all possible levels appear in the list. The remaining part of the sum is estimated by assuming a hydrogenic structure and accounting for the different multiplicity of these levels from the hydrogenic statistical weights. The maximum orbital quantum number is given in equation (4.5) and the statistical weight for hydrogenic levels is given by

$$g^{\text{hyd}}(n) = 2 \sum_{l=0}^{n-1} (2l+1) = 2n^2 \quad (4.6)$$

This leads to the expression for the internal partition function

$$B_{i-1}(T_e) \approx \sum_{p=1}^{n^1} g_{i-1}(p) \exp \left\{ - \frac{E_{i-1}(p)}{kT_e} \right\} + \quad (4.7)$$

$$+ (2S_1+1)(2L_1+1) \sum_{p=n^1+1}^{n_{\text{max}}} 2p^2 \exp \left\{ - \frac{E_{z-1}(\infty) - \frac{i^2 E_H}{p^2}}{kT_e} \right\}$$

where n^1 is the maximum orbital quantum number found in the table

3.5 The plasma pressure

The independent variables chosen were the number densities and the electron temperature. They were selected because they do not have to be corrected when the density of the plasma is high. From the expressions for the free energy from Sections 3.3 and 3.4 it is possible to derive a formula relating the pressure to these variables. There will be a high-density correction to the pressure, and that is why it was not chosen to be an independent variable (reference [40]).

The pressure, p , is directly related to the free energy through the thermodynamic relation

$$p = - \frac{\partial}{\partial V} (FV) \quad (5.1)$$

where the free energy consists of two parts (equation (3.4))

$$F = F_0 + F_{\text{coul}} \quad (5.2)$$

that is, the sum of the free energy of a system with negligible interactions and the free energy in the Coulomb interaction (Section 3.4). The first of these will give the ordinary kinetic pressure or ideal gas pressure

$$p_0 = kT_e (n_e + \sum_i n_i) \quad (5.3)$$

The coulombic part of the free energy will cause a slight decrease in the pressure, because of the attraction between charges of different signs. As said earlier, particles with charges of opposite sign tend to be closer together on the average than particles with charges of the same sign. This correction is given by

$$\Delta p = - \frac{\partial}{\partial V} (F_{\text{coul}} V) = - F_{\text{coul}} - V \frac{\partial F_{\text{coul}}}{\partial V} \quad (5.4)$$

4. THE CALCULATION OF THE COMPOSITION OF A NITROGEN SPARK

The theory presented in Chapter 3 will now be used to compute some of the quantities of interest for a real nitrogen spark plasma. In the first section of this chapter the Saha equation is used together with the conditions of mass and charge conservation to derive the expressions for the number densities of atoms and up to triply ionized ions. These expressions are substituted back into the conservation of mass relation to arrive at an implicit expression for the electron temperature when the electron and the particle number densities are known, and from the electron temperature the composition of the spark can be calculated. But in order to do this, the way in which the internal partition functions in the Saha equation are calculated must be improved compared with the method presented in Section 3.4. Such an improved method is presented in Section 4.2. The amount of molecular nitrogen in the spark has so far been assumed to be negligible, but if the pressure is very high or the temperature low, there may be a significant fraction of nitrogen molecules present. The equilibrium relation for dissociating nitrogen is therefore presented in the third section. Finally, the material in the preceding sections is assembled into a procedure to calculate the electron temperature and plasma composition of a nitrogen spark, and this is applied to the measurements made by Aldén et al. and the results of the computations are presented and discussed.

$$\sum_{s=1}^n A_s + 1$$

where the additional unknown is the electron density. For each species the number of Saha equations is $A_s - 1$, and together with a conservation of mass relation for the species this will give

$$\sum_{s=1}^n A_s$$

equations altogether. The condition of macroscopic neutrality gives the final relation necessary to determine all the unknown number densities.

The general solution to the system yields the number densities in A_s different ionization stages of n different chemical species. Since the calculations in this work are performed for a spark in nitrogen, only the expressions for a single species will be needed. The relations for the number densities for a single species ionized up to three times are

$$n_0 = \frac{n_e^4}{K_0 S(T)} \quad (1.4a)$$

$$n_1 = \frac{n_e^3}{S(T)} \quad (1.4b)$$

$$n_2 = \frac{K_1 n_e^2}{S(T)} \quad (1.4c)$$

$$n_3 = \frac{K_1 K_2 n_e}{S(T)} \quad (1.4d)$$

where

$$S(T) = n_e^2 + 2K_1 n_e + 3K_1 K_2 \quad (1.5)$$

The starting expression for the internal partition function for an atom or an ion is

$$Q = g_0 + \sum_{i=1}^P Q^i \quad (2.1)$$

where Q^i is the contribution to the partition function from the electron configuration belonging to the i :th parent ion excited state

g_0 is the statistical weight of the ground state

P is the number of different parent ion states considered

The Q^i terms are expressed as a sum over k states with statistical weight g_j and excitation potential χ_j , and an asymptotic hydrogen-like tail

$$Q^i = \sum_{j=1}^k g_j 10^{-\chi_j \theta} + 2g_{pr} Q_{as}(1, z) 10^{-\chi_{ion} \theta} \quad (2.2)$$

where θ is the inverse temperature, in electron volts, connected to the electron temperature through the relation

$$\theta = \frac{5040}{T_e} \quad (2.3)$$

g_{pr} is the statistical weight of the parent ion:

$$g_{pr} = (2S+1)(2L+1) \quad (2.4)$$

z is the effective nuclear charge; $z=1$ for neutral atoms etc.

l is an effective quantum number which is tabulated in Traving et al. [41]

χ_{ion} is the ionization energy in eV

$$f(\theta) = \sum_{j=1}^k g_j 10^{-\chi_j \theta} \quad (2.9)$$

is calculated by Traving et al. and then they make a fit to a sum of exponential terms (Chebyshev polynomial) by adjusting the parameters. In mathematical symbols

$$f(\theta) \approx \phi(\theta) = \sum_{v=1}^m \alpha_v 10^{-\gamma_v \theta} \quad (2.10)$$

where the number of terms, m , is between 2 and 5. A considerable reduction in the number of terms in the summation is thus achieved. The parameters α_v and γ_v are chosen so that the sum will be a good approximation to a direct summation of the values in the table of Moore (reference [39]).

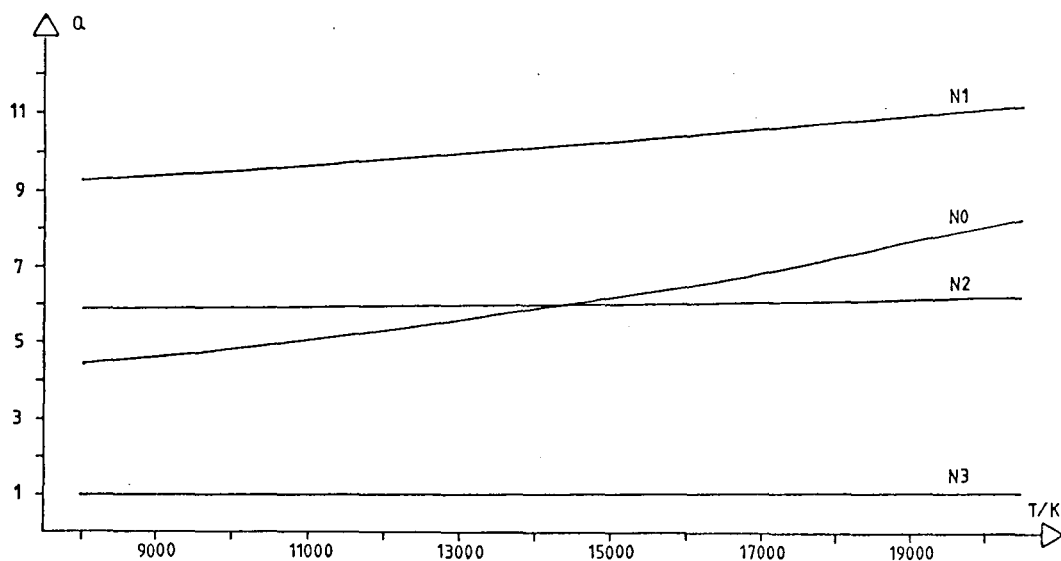


Figure 2.1. The internal partition functions versus temperature for nitrogen atoms and ions with charges from -1 to -3 calculated with the method described in this section.

The values of the parameters appearing in the calculation of the internal partition function for nitrogen according to this method are presented in Table 2.1.

According to Traving et al. the approximation in equation (2.10) is valid for temperatures obeying the condition

$$T > 6.3 \cdot \chi_{\text{ion}} \quad (2.11)$$

where χ_{ion} has the unit eV

in the sense that the maximum error is then less than 1 %. This condition holds for the temperatures of interest in this work.

The values calculated with this method for nitrogen are presented in Figure 2.1. The value of the inner partition function in this figure depends weakly on the composition through the lowering of the ionization energy in formula (2.7).

4.3 Calculation of the nitrogen dissociation equilibrium

So far it has been assumed that the nitrogen molecules in the gas are initially dissociated into atoms. This is a reasonable assumption for the temperatures which are found in a spark. Nitrogen is completely dissociated into atoms for temperatures higher than 10000 K, if the pressure is atmospheric. However, if the pressure is considerably higher than this (as will be shown to be the case) there will be an appreciable amount of molecules present in the spark. The calculation of this molecular number density under the assumption of L.T.E. will be treated in this section.

where p is the total pressure

The total partition function, Q , for a molecule can be decomposed into 4 factors; a translational, a vibrational, a rotational and an electronic part

$$Q = Q_t Q_v Q_r Q_e \quad (3.6)$$

The second equilibrium constant that can be of use in treating the chemical equilibrium (3.1) is called the pressure equilibrium constant, K_c , defined in terms of the concentrations, $n(X)$, of the species involved in the reaction

$$K_c = \frac{\prod_i n^{b_i}(B_i)}{\prod_i n^{a_i}(B_i)} \quad (3.7)$$

For K_c a relation analogous to (3.3) holds, where the partition function for the standard state of unit pressure is replaced by the partition function for the standard state of unit concentration, Q_c , which is related to the total partition function by

$$Q_c = \frac{p}{RT} Q \quad (3.8)$$

From equations (3.3), (3.4) and (3.8) it can be seen that the relation between the two equilibrium constants is

$$K_c = K_p (RT)^{\sum a_i - \sum b_i} \quad (3.9)$$

In Hansen [42] the explicit expressions for the pressure equilibrium constant of the nitrogen dissociation reaction and also the partition functions of nitrogen molecules and atoms are given. The pressure equilibrium constant is

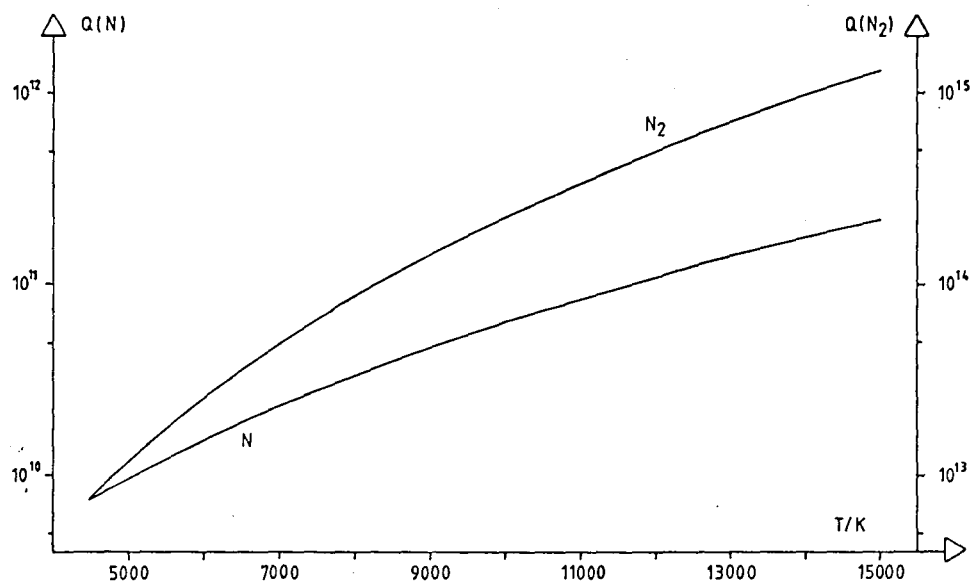


Figure 3.1. The partition functions for nitrogen molecules and atoms according to the formulae above (logarithmic scales) versus temperature.

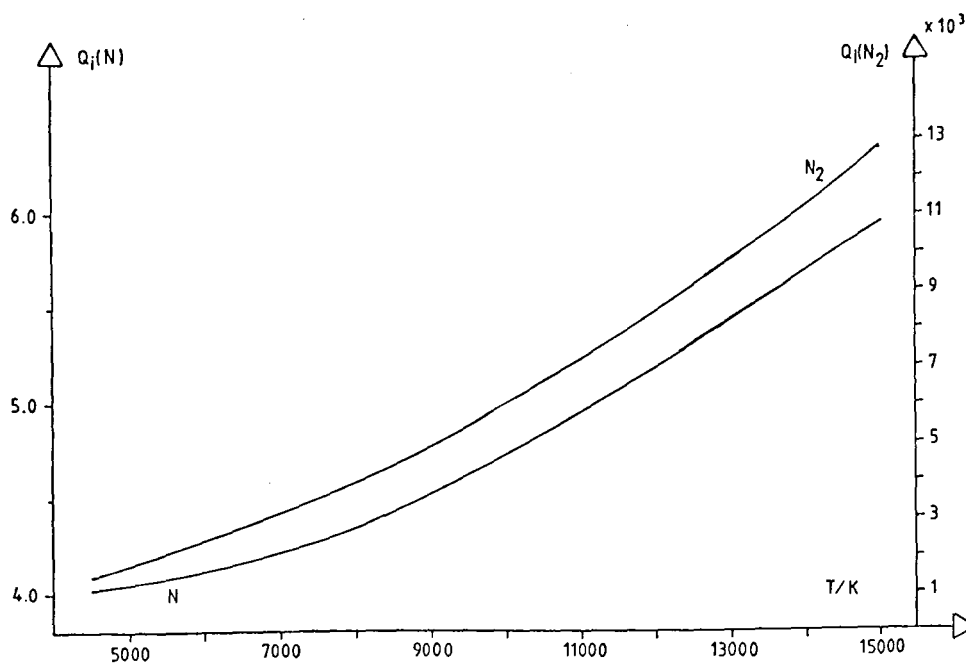


Figure 3.2. The inner part contribution to the partition functions for molecular and atomic nitrogen in Figure 3.1.

The quantity ϵ is plotted in Figure 3.4 as a function of the temperature for various pressures.

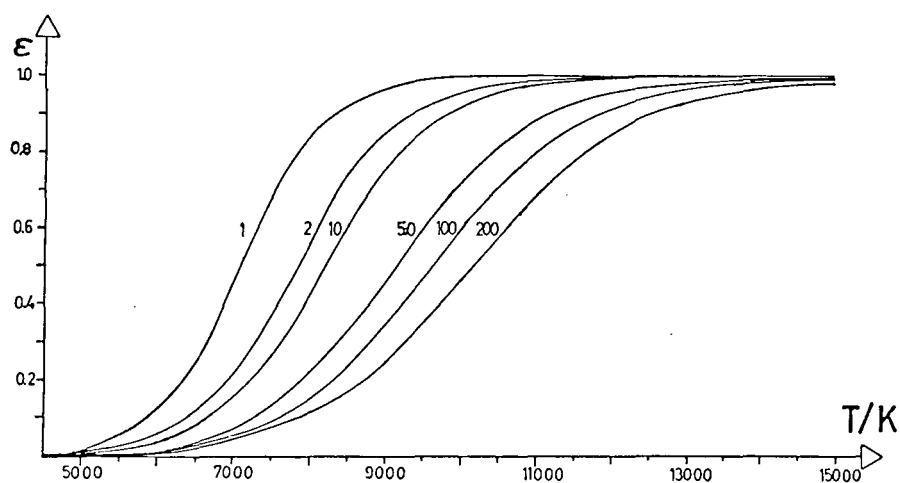


Figure 3.4. The fraction of molecules which have dissociated into atoms versus temperature for different values of the pressure in atmospheres.

It should be noted that at high pressure the fraction of nitrogen molecules can be very high, as stated at the beginning of this section.

The relation between ϵ and the number densities of molecules and atoms is found by using the definition of ϵ .

$$\epsilon = \frac{n_m^0 - n_m}{n_m^0} \quad (3.17)$$

where n_m^0 is the number density of molecules before dissociation

and the obvious relation

$$n_m^0 = n_m + \frac{n_0}{2} \quad (3.18)$$

Eliminating n_m^0 from the two relations above yields

$$\Delta N = -n_u + R (n_0 + n_1 + \dots) \quad (4.1)$$

the sum within the parantheses is equivalent to the particle density, NA, in equation (1.6):

$$NA = \frac{n_e}{S(T)} \left(\frac{n_e^3}{K_0} + n_e^2 + K_1 n_e + K_1 K_2 \right) \quad (4.2)$$

where, (equation (1.5))

$$S(T) = n_e^2 + 2K_1 n_e + 3K_1 K_2 \quad (4.3)$$

Combining formulae (4.2) and (4.3) gives the implicit equation for the electron temperature

$$NA = \frac{\Delta N + n_u}{R} = \frac{n_e}{S(T)} \left(\frac{n_e^3}{K_0} + n_e^2 + K_1 n_e + K_1 K_2 \right) \quad (4.4)$$

where n_u is calculated from equation (2.1.6)

K_i is the right hand-side of the Saha equation,
expression (3.3.20):

$$K_i = 2 \left(\frac{2\pi m_e kT_e}{h^2} \right)^{3/2} \frac{B_i(T_e)}{B_{i-1}(T_e)} \exp \left\{ - \frac{E_{i-1}(\infty) - \Delta E_{i-1}(\infty)}{kT_e} \right\} \quad (4.5)$$

where the lowering of the ionization energy is given by equation (3.3.21)

$$\Delta E_{i-1}(\infty) = \frac{i e^3}{4\pi\epsilon_0} \left(\frac{n_e + \sum_i i^2 n_i}{kT_e} \right)^{3/2} \quad (4.6)$$

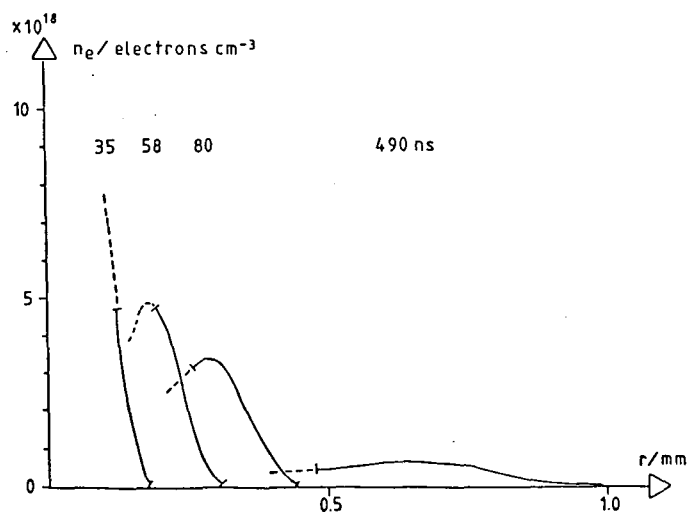


Figure 4.1. The parts of the curves in Figure 2.4.1 which were used in the calculations.

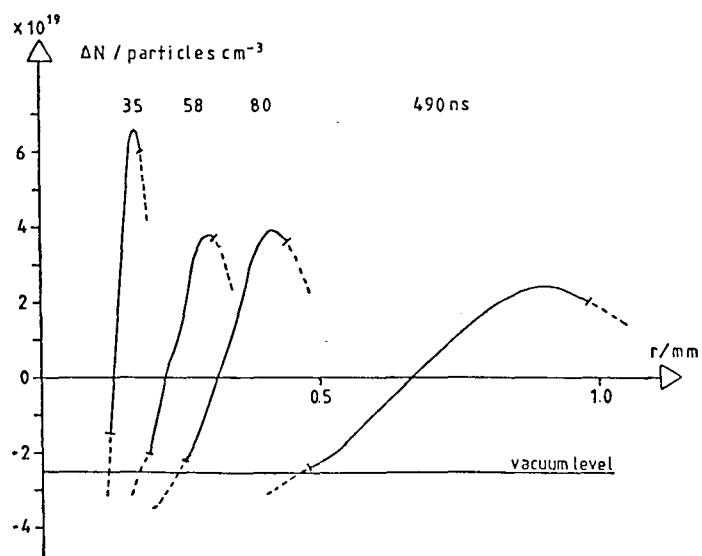


Figure 4.2. The parts of the curves in Figure 2.4.2 which were used in the calculations.

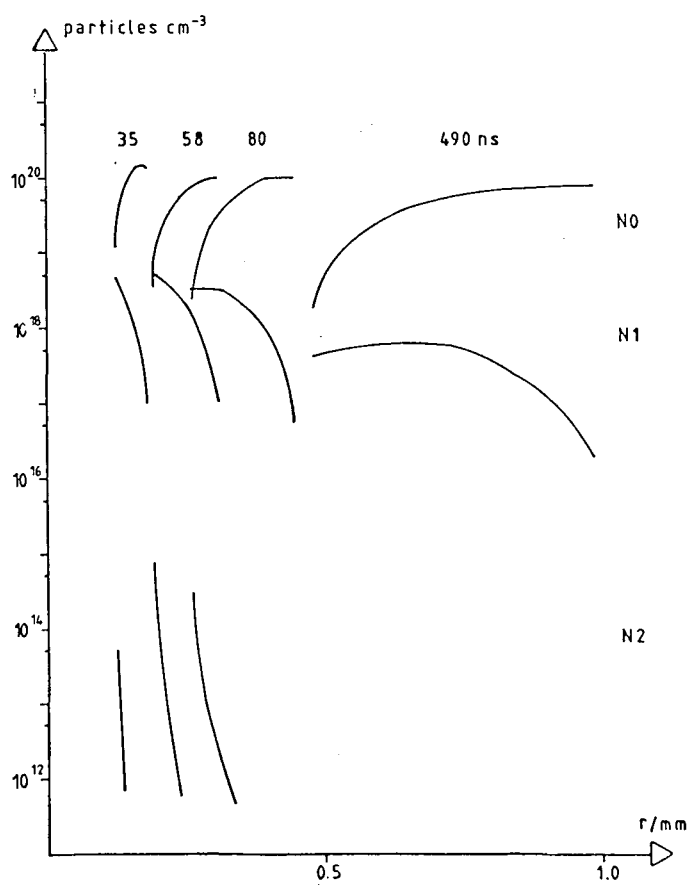


Figure 4.4. The number density (logarithmic scale) for atoms and singly and doubly ionized nitrogen versus radius for different times in nanoseconds.

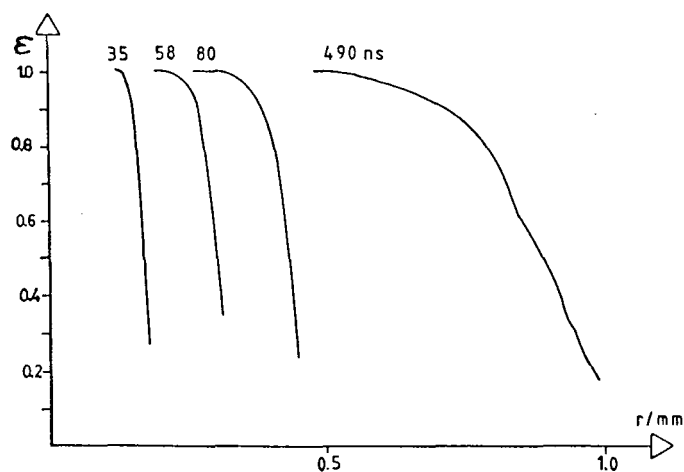


Figure 4.6. The fraction of molecules which are dissociated versus radius for different times in nanoseconds.

The dissociation equilibrium should therefore be included in the computations. This is done in the following way. In the procedure above, the electron temperature and the pressure are determined. Then it is possible to determine the fraction of molecules that have dissociated into atoms, ϵ , from equation (3.16). The value of ϵ is used in equation (3.19)

$$N_A = \frac{2\epsilon}{1-\epsilon} n_m \quad (4.8)$$

to determine the relation between the number densities of atoms and molecules. The atom number density is now denoted by N_A because it will subsequently be used in the computation of the ionization equilibrium. Substituting this expression into formula (2.4.4)

$$\Delta N = n_m - n_u + R N_A \quad (4.9)$$

gives the expression for the molecular number density as

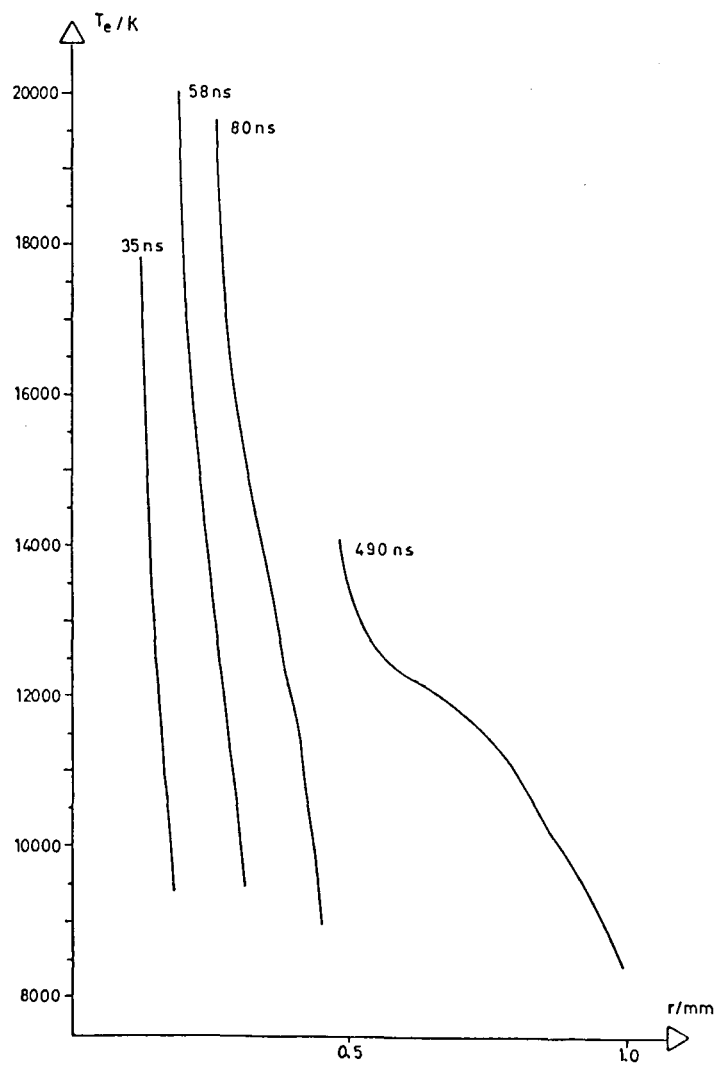


Figure 4.7. The electron temperature versus radius for different times in nanoseconds, calculated with the presence of molecules taken into account.

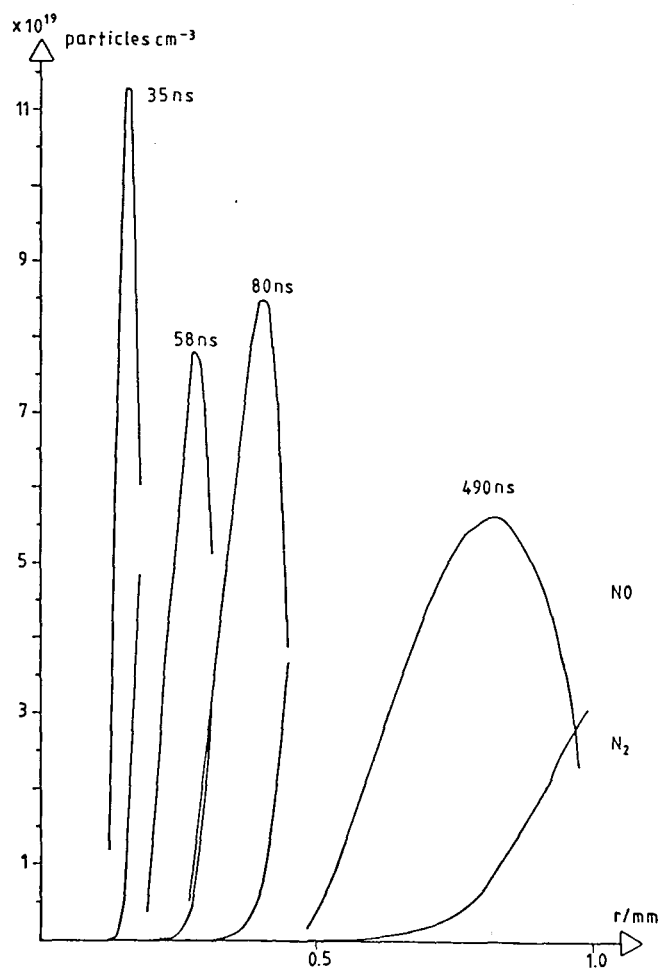


Figure 4.9. The number density for molecules and atoms versus radius for different times in nano-seconds, from Figure 4.8.

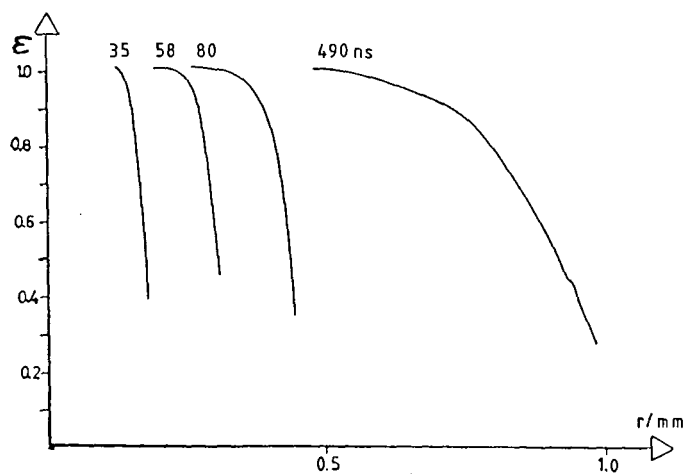


Figure 4.11. The fraction of molecules which are dissociated versus radius for different times in nanoseconds, calculated with the presence of molecules taken into account.

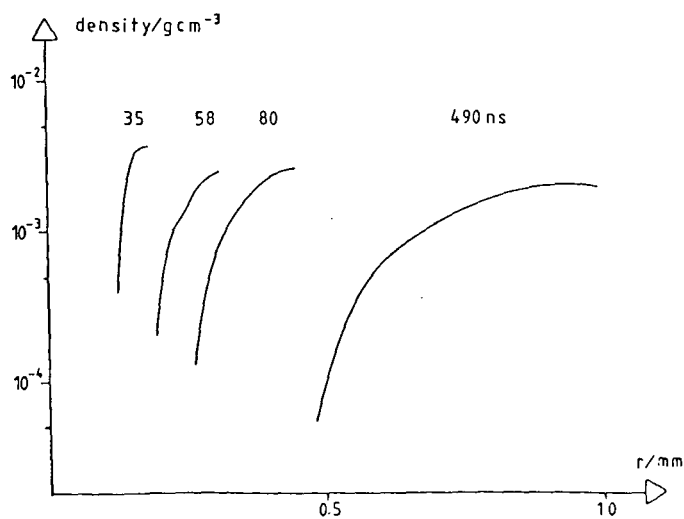


Figure 4.12. The density (logarithmic scale) versus radius for different times in nanoseconds, calculated with the presence of molecules taken into account.

For comparison the number density and density curves calculated for a nitrogen plasma with a pressure of one atmosphere are shown in Figure 4.14.

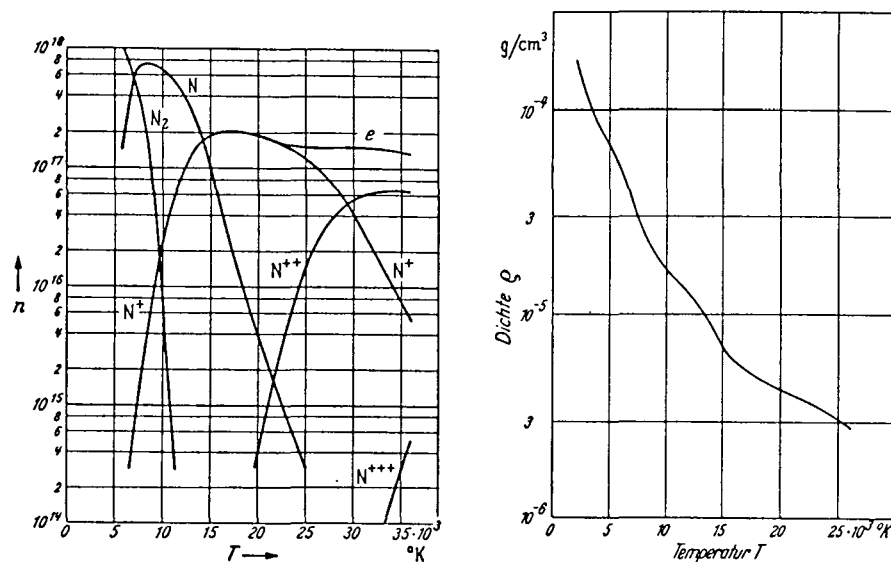


Figure 4.14. The number density and density for a nitrogen plasma with a pressure of one atmosphere, taken from reference [46].

The influence of the uncertainties in the experimental values on the results of the computations was estimated by adding the statistical error reported by Aldén et al. of the electron density: 2×10^{17} to the electron density and subtracting 10 times this value from the particle density and then performing the calculation with these input-values, and then repeating the calculation with the signs of the changes reversed. The reason for this was that these should represent the warmer and colder boundary cases of the uncertainty. The effect of the changes on the pressure, the temperature and the density was typically below 5%, with some exceptions at the end of the curves up to 20%. The deviations in the figures these changes would cause would be less than the thickness of the curve for the majority of the evaluated points.

different and the expression for the diffusion length is stated in Section 5.5. In the last section some of these conditions are applied to the results presented in Section 4.4.

5.1 General validity criteria for L.T.E.

In this section some general criteria for L.T.E. will be considered. The first and most important is that the electron-electron relaxation time should be shorter than any other characteristic time of the plasma. Then the free electrons are in thermal equilibrium with each other, i.e. they have a maxwellian velocity distribution. The relaxation time for electron-electron collisions, t_{ee} , is given by Spitzer (reference [12]) in a fully ionized hydrogen plasma as

$$t_{ee} = 0.226 \frac{T_e^{3/2}}{n_e \ln \Lambda} \quad (1.1)$$

where Λ is a slowly varying function of n_e and T_e ; for $n_e \sim 10^{18} \text{ cm}^3$ and $T_e \sim 10^4 \text{ K}$ $\ln \Lambda$ is roughly equal to 5.

The value of the relaxation time is plotted in Figure 1.1 as a function of the electron temperature when Λ is assumed to be constant.

From the figure it can be seen that the relaxation time is very short, and, consequently, the free electrons do have a maxwellian velocity distribution in almost all laboratory plasmas.

and the relaxation time between ions and electrons as

$$t_{ie} \approx (7.5 \times 10^{-7} \left(\frac{i^2 E_H^2}{kT_e}\right)^{3/2} n_e)^{-1} i \frac{M_a}{m_e} \quad (1.3)$$

where $i=1$ for singly charged ions, $i=2$ for doubly charged ions etc.

The order of magnitude of these two times suggests that the kinetic temperatures do not deviate from each other significantly, even in a transient plasma, if it is in L.T.E.. The time for equilibration between heavy particles is less than the electron-particle relaxation time (reference [4]).

Finally, the effect of the applied electric field on the equilibrium is examined. The condition that the electric field should not cause the electron temperature to be different from the particle temperature is that the energy gained by the electrons from the applied field should be small over their mean free path, and that it should also be smaller than the energy that can be transferred to heavier particles. If only single ionized atoms are assumed to be present, this requires that the external electric field obeys the condition

$$E^2 \ll (5.5 \times 10^{-12} n_e \frac{E_H}{kT_e})^2 \frac{m_e}{M_a} \quad (1.4)$$

taken from reference [4].

5.2 Criteria for the validity of partial L.T.E. in a homogeneous and time-independent plasma

In a homogeneous and time-independent plasma with small optical depth the reabsorption of radiation can be neglected. To recapitulate, for the plasma to be in a state of L.T.E. the collisional population and depopulation rates have to be considerably greater than the rates

If the minimum electron density for at least one level below the reduced ionization limit is less than the actual electron density, it is implied that the free electrons have a thermal velocity distribution, if the time variations or the spatial variations of the electron temperature are not too great.

5.3 Criteria for the validity of complete L.T.E. in a homogeneous and time-independent plasma

In the preceding section a condition for an excited state to be in local equilibrium with all higher states was presented. This condition is not applicable, as it stands, for lower excited states, and especially for the ground state where the deviations from hydrogenic behaviour are more substantial. Griem states that it is only the equilibrium between the ground state and the upper level of the resonance line that then needs to be investigated to decide if complete L.T.E. exists. The relevant condition is that the radiative population rate of the ground state should be negligible compared with the collisional population rate of the same level. Near L.T.E., both of these rates is dominated by transitions from the upper level of the resonance line. Comparing the population rate by radiative transitions with the population rate by collisional transitions, and assuming that the population distribution over these two levels is thermal, he shows that complete L.T.E. in an optically thin plasma may be expected if the electron density fulfils the inequality

$$n_e \geq 9 \times 10^{17} \left(\frac{E_{i-1}(2) - E_{i-1}(1)}{E_H} \right)^3 \left(\frac{kT_e}{E_H} \right)^{1/2} \text{ [cm}^{-3}\text{]} \quad (3.1)$$

The condition utilized in arriving at this formula is, as in the previous section, that the collisional rate should be ten times greater than the radiative rate. This expression is valid for hydrogen and hydrogenic ions, but it can also be used to estimate minimum electron densities for L.T.E. for other chemical species because of the cancellation of some specific hydrogen quantities in the

$$n_e \geq 5.6 \times 10^{17} \left(\frac{kT_e}{E_H} \right)^{1/2} \left(\frac{E_{i-1}^{(\infty)}}{E_H} \right)^3 \quad [\text{cm}^{-3}] \quad (3.3)$$

Note that this expression contains the ionization energy instead of the energy difference of the first resonance line. This condition is more severe than equation (3.1) and it should be used when low excited states exist. If, as before, the resonance radiation is absorbed the condition expressed in equation (3.3) may be relaxed an order of magnitude.

5.4 Criteria for the validity of complete L.T.E. in a homogeneous and transient plasma

Plasmas that have sufficiently high electron density to be in L.T.E. are rarely both homogeneous in time and space. In this section the validity criteria for a plasma which is transient but essentially homogeneous in space, for instance plasmas produced in shock-tubes, will be stated.

The necessary condition for the plasma, in addition to the criteria in the preceding sections, is that the change in the electron temperature should be small over the time characterizing the establishment of excitation and ionization equilibrium. The mechanism for collisional ionization is through a succession of excitations into intermediate states and not by direct ionization, if the plasma goes through a sequence of quasi-stationary near-L.T.E. states. Thus the relaxation time is determined by the slowest step in the chain, that is, by the inverse collisional-excitation rate of the ground state per atom (or ion) multiplied by the number of atoms that is to be excited or ionized. The majority of the excitations is to the upper level of the resonance line, and assuming a Maxwellian velocity distribution for the free electrons, the relaxation time is then estimated by

The electron densities for a transient plasma to be in L.T.E. are quite high. A reduction in the necessary concentration such as the one in Section 5.3 is not allowed in this case, because self-absorption of the resonance line does not lead to any reduction in the equilibrium time as it does not cause any net change in the excitation rate in an isolated, homogeneous plasma. On the other hand, the time required to establish partial L.T.E. is much shorter than the time required for complete L.T.E., so that the transient nature of a plasma only rarely causes deviations from partial L.T.E., if it had existed in a stationary, homogeneous plasma. The expression for the equilibrium time in this case is given by equation (6-67) in Griem (reference [4]).

As pointed out before, the criterion (4.1) gives fairly long relaxation times, too long for complete L.T.E. to exist in most transient plasmas. However, this criterion is too pessimistic in the case of a decaying spark, since it accounts only for collisional ionization. The spark, where radiative excitation and ionization are important, will require another, less severe, criterion. In this case, the relevant recombination time is very short (reference [4]), that is, the relaxation from the initial non-equilibrium state to L.T.E. will be very rapid. So rapid that the decisive condition for a decaying plasma will be the same as the one for a time-independent and homogeneous plasma. When the plasma is in the build-up state, i.e. the period when the ionization is increasing, L.T.E. should rarely prevail.

5.5 Criteria for the validity of complete L.T.E. in an inhomogeneous and time-independent plasma

In the previous section it was established that it takes a certain time $\tau_{i-1}(1)$ for the plasma to attain a state of local equilibrium. If the plasma is inhomogeneous it is necessary that the spatial variation of the electron temperature be small over the distance that a given particle can diffuse in that time, in order not to disrupt the equilibrium. When the density of molecules is negligible, this

where A_a is the atomic weight of species a.

The criterion for L.T.E. in this case is

$$\frac{T_e(r) - T_e(r+d)}{T_e(r)} = \delta \ll 1 \quad (5.5)$$

and, as in the preceding section, the difference between the excitation or ionization temperature and the free electron temperature may be estimated to be

$$T_e - T_{ex} = \delta T_e \quad (5.6)$$

If the value of δ is in the ten percent range, then deviations from L.T.E. must be expected, but still the excitation and ionization equilibrium can be determined by some average value of the electron temperature over the diffusion distance d .

In the outer, cold, zones of a plasma the value of d is larger than that calculated in equation (5.4), because ions and excited atoms diffuse from the hot inner zones, and thereby reduce the required rate of electron collision excitations from the ground state. But, as in the case of a transient plasma, rapid relaxation from a non-equilibrium state takes place. Also, the intense resonance radiation from the inner zones might help to establish equilibrium in the outer zones. However, the trapping of resonance radiation in the inner zones does not increase the net rate of excitation.

5.6 Application of the criteria to the sparks in nitrogen

The expression presented in the preceding sections will now be applied to the sparks in a nitrogen atmosphere to ascertain whether the assumption of L.T.E. is valid for them. The results presented in Section 4.4 are used in the computations.

fulfilment of this condition is ensured for the sparks.

Application of the condition in equation (4.1) to investigate the effect of the transient nature of the sparks gives very long relaxation times for the nitrogen atoms. These times are plotted in Figure 6.2 where the same resonance line as before has been used, and its oscillator strength value, $f_{21}=0.00242$, is taken from reference [4].

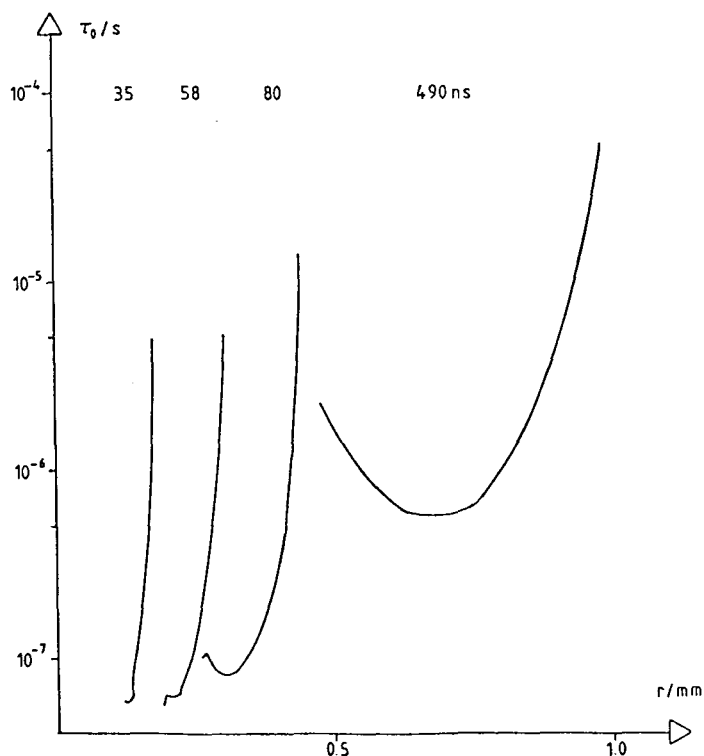


Figure 6.2. Relaxation times calculated with formula (4.1) for atoms (logarithmic scale) versus radius for different times.

The discussion at the end of Section 5.4 about this estimate being too pessimistic for a decaying plasma may be applicable here, so the spark is probably in complete L.T.E., at least for the two longer times. The question of whether it is in L.T.E. or not due to transient effects will probably be answered when more experimental data have been evaluated. Note that it is the relaxation time for atoms which has been calculated. The rapid increase in the minimum electron concentration with increasing ionization in this transient case

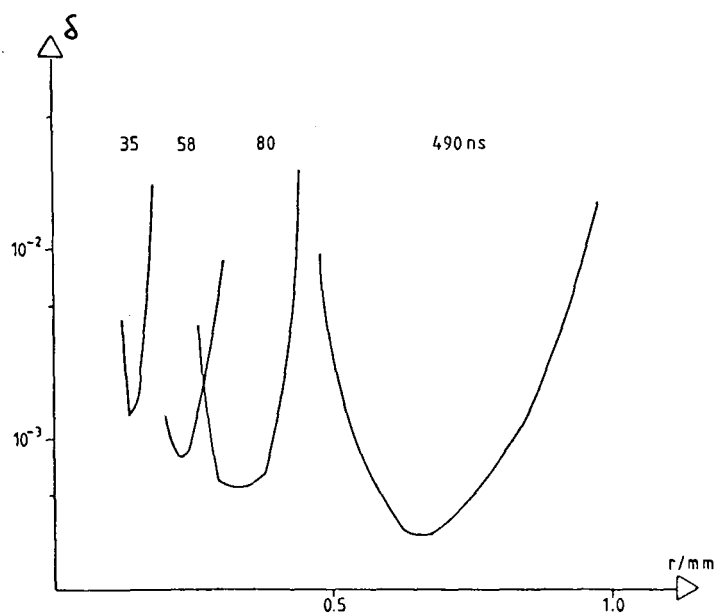


Figure 6.4. The relative difference between the ionization temperature and the electron temperature calculated from equation (5.5) (logarithmic scale) versus radius for different times.

Finally, it should be emphasized that the expressions and discussions in this chapter have dealt solely with the case of a totally dissociated plasma. How the assumption of L.T.E. should be verified when there is a significant amount of molecules present in the plasma is outside the knowledge of the author.

7. REFERENCES

1. Aldén et al. Int. Symp. Diag. Mod. Comb.
Recipr. Eng.
September 4-6, 1985
Tokyo p. 85
2. Kunkel (ed.) "Plasma Physics in Theory and
Application"
McGraw-Hill, 1966
3. Nilsson "Plasmafysik"
avd. för Matematisk Fysik, Lund
4. Griem "Plasma Spectroscopy"
McGraw-Hill, 1962
5. Marr "Plasma Spectroscopy"
Elsevier, 1968
6. Cooper Rep. Prog. Phys., 29, 35 (1966)
7. Lochte-Holtgreven "Plasma Diagnostics"
(ed.) North-Holland, 1968
8. Huddleston and "Plasma Diagnostic Techniques"
Leonard (eds.) Academic Press, 1965